



Prognostic significance of PD-L1 expression and CD8⁺ TILs density for disease-free survival in surgically resected lung squamous cell carcinoma: a retrospective study

Xiaomin Cheng^{1,2^}, Lei Wang¹, Zhemin Zhang¹

¹Department of Medical Oncology, Shanghai Pulmonary Hospital and Thoracic Cancer Institute, School of Medicine, Tongji University, Shanghai, China; ²School of Medicine, Tongji University, Shanghai, China

Contributions: (I) Conception and design: X Cheng, Z Zhang; (II) Administrative support: Z Zhang; (III) Provision of study materials or patients: L Wang; (IV) Collection and assembly of data: X Cheng, L Wang; (V) Data analysis and interpretation: X Cheng; (VI) Manuscript writing: All authors; (VII) Final approval of manuscript: All authors.

Correspondence to: Professor Lei Wang; Professor Zhemin Zhang. Department of Medical Oncology, Shanghai Pulmonary Hospital and Thoracic Cancer Institute, School of Medicine, Tongji University, No. 507, Zheng Min Road, Shanghai 200433, China.

Email: wangleixxn@163.com; zhemin.doc@163.com.

Background: This study sought to depict the genomic landscape of patients with surgically resected lung squamous cell carcinoma (LUSC) and its relationship with clinical outcome indicators.

Methods: We retrospectively collected the clinical data of 180 patients from the electronic medical records and applied targeted sequencing and immunohistochemistry (IHC) to depict the genomic landscape, including the tumor mutation burden (TMB), programmed cell death-ligand 1 (PD-L1), and cluster of differentiation CD8⁺ tumor-infiltrating lymphocytes (CD8⁺ TILs). And comparative analysis and survival analysis of these parameters were conducted to find prognostic factors for clinical outcome.

Results: PD-L1+ tumor cells were observed in 75 (41.7%) of the patients, the median rate of CD8⁺ TILs was 11.5 [4, 24], and the median TMB was 9.4 (7.5–13.7) mutations per megabase (mut/Mb). Patched receptor 1 (*PTCH1*) gene mutation frequency was significantly associated with CD8⁺ TILs density (12% *vs.* 1%; *P*=0.024). High PD-L1 expression and CD8⁺ TILs+ were significantly associated with longer disease-free survival (DFS), and a further subgroup analysis revealed that both were significantly correlated with the DFS of stage I/II patients but not stage III patients.

Conclusions: The results suggest that only *PTCH1* gene mutation frequency was correlated with CD8⁺ TILs density. Additionally, intense CD8⁺ TILs density and high PD-L1 expression were found to be associated with longer DFS. Our findings provide insights into the precise treatment strategy for surgically resected LUSC patients.

Keywords: CD8⁺ tumor-infiltrating lymphocytes (CD8⁺ TILs); programmed cell death-ligand 1 (PD-L1); lung squamous cell carcinoma (LUSC); immunotherapy

Submitted Apr 14, 2022. Accepted for publication Jun 09, 2022.

doi: 10.21037/jtd-22-630

View this article at: <https://dx.doi.org/10.21037/jtd-22-630>

Introduction

Lung squamous cell carcinoma (LUSC) is one of the most common pathological types of non-small cell lung cancer

(NSCLC) and remains the leading cause of tumor-related deaths globally (1,2). Unlike lung adenocarcinoma (LUAD), which has oncogenic driver changes, the treatment for LUSC made little progress and conventional platinum-based

[^] ORCID: 0000-0002-0352-3961.

chemotherapy remains the gold standard treatment (3-5). The gold standard for early LUSC treatment is lobectomy with peripheral lymph node dissection (3). However, the recurrence rate within 5 years after standard treatment is still more than 20% (5). Although adjuvant chemotherapy only provided a limited survival benefit (6), complete resection surgery combined with adjuvant chemotherapy was the optimal treatment for prolonging survival. Recently, neoadjuvant and adjuvant using immune checkpoint inhibitors (ICIs) has shown promising results. ICIs targeting programmed cell death protein 1 (PD-1) and its ligand (PD-L1), compared to conventional chemotherapy, have prolonged survival, and the treatment of advanced lung cancer has been brought into a new era (7-10). A preliminary study (11) found that neoadjuvant nivolumab caused 45% of patients to have primary pathological response in early lung cancer.

Tumor mutation burden (TMB) was found having no relationship with pathologic response of neoadjuvant Atezolizumab in the LCM3 study (12), while the response could also be found in patients with negative PD-L1 expression. Multiple retrospective studies (13-15) suggest that the disease-free survival (DFS) may be related to the differentiation and abundance of various immune cells in tumor tissues of LUSC patients. tumor-node-metastasis (TNM) stages (16,17) can predict the prognosis of LUSC, but its accuracy remains unclear. Previous studies (12,18,19) have shown that age, gender, smoking location and so on have certain limitations in predicting DFS of early stage LUSC after surgery. Therefore, it is necessary to comprehensively delineate the genomic landscape and immune pattern of lung cancer patients and elucidate their correlations to illuminate the phenotypes of lung cancer patients that could potentially benefit from immunotherapy, which could facilitate the development of neoadjuvant immunotherapy strategies for NSCLC patients. Several studies have reported data on LUAD, though, situations of LUSC remains largely unknown currently (20,21).

In this study, we reviewed 180 patients underwent completely resection of LUSC without any history of immunotherapy and analyzed the correlations among the TMB, PD-L1 expression, cluster of differentiation 8⁺ tumor-infiltrating lymphocyte (CD8⁺ TILs) density, and other clinical parameters with the genomic landscape and survival. We present the following article in accordance with the REMARK reporting checklist (available at <https://jtd.amegroups.com/article/view/10.21037/jtd-22-630/rc>).

Methods

Sample collection

Retrospectively, we reviewed the data of 180 patients with histologically confirmed LUSC that had undergone surgical resection of the lung (lobectomy or pneumonectomy), who had not previously received any immunotherapy, at the Shanghai Pulmonary Hospital from 2013 to 2016. Samples with insufficient or poor quality, missing baseline clinicopathological features, mixed histology, or incomplete follow-up data were all excluded. We confirmed the histological type of each case in the medical electronic records. Corresponding formalin-fixed and paraffin-embedded (FFPE) tissues were used for whole-exome sequencing (WES) and immunohistochemistry (IHC) staining. Tissues were used for WES and IHC. Patients' baseline characteristics were collected, including age, sex, smoking history, Eastern Cooperative Oncology Group performance status (ECOG PS), tumor maximum diameter, lymph node status and stage, pleural invasion status, vascular invasion status, tumor TNM stage, differentiation degree, chemotherapy regimens and tumor location classification, which were used to test whether the baseline features were biased. We also collected the data of disease free survival (DFS) and overall survival (OS) to analyse the association between biomarkers and prognosis. Survival status and data were followed through telephone and the follow-up time ended on January 31, 2022. Stage TNM was defined with the eighth UICC/AJCC TNM classification (22) and radiographic progression disease (PD) were defined according to the Response Evaluation Criteria in Solid Tumors (RECIST), version 1.1 (23). DFS refers to the time since initial surgical resection until recurrence. OS is calculated from the date of diagnosis of LUSC to death from any cause or to censoring at the last follow-up visit. This study was conducted in accordance with the provisions of the Declaration of Helsinki (as revised in 2013) and was approved by the Ethics Committee of Shanghai Pulmonary Hospital (No. K20-288). Individual consent for this retrospective analysis was waived.

PD-L1 expression

Anti-human PD-L1 antibody (#13684, clone E1L3N, Cell Signaling Technology, Danvers, MA, diluted 1:200) was used to determine PD-L1 expression in accordance with the manufacturer's recommendations. PD-L1

expression was defined as the percentage of tumor cells showing membranous immunoreactivity (in the central or marginal tumor region). The samples were also retested using another antibody assay (24) (clone SP142, Spring Bioscience, Ventana, Tucson, AZ, diluted 1:100). The cutoff value for dichotomizing PD-L1 positivity or negativity (PD-L1+/-) was 1%. Sections of human placenta tissues and the breast cancer cell line MCF-7 were employed as the positive and negative controls for the PD-L1 IHC staining, respectively.

CD8⁺ TILs density

The CD8⁺ TILs density was assessed using a mouse anti-CD8 monoclonal antibody (clone C8144B, DAKO). These lymphocytes contain the CD8 cytoplasmic marker and infiltrate within tumor regions (central or marginal) were defined as CD8⁺ TILs. Similar to the approach adopted by previous studies (25,26), we identified positive/negative CD8⁺ TILs density (CD8⁺ TILs+/-) with a cutoff value of 0%.

Targeted sequencing and TMB calculation

All Genomic deoxyribonucleic acid (DNA) samples included in this study were extracted using the Qiagen DNeasy FFPE DNA Kit (Qiagen, Hilden, Germany) according to the manufacturer's instructions, and a DNA library was constructed. The matched peripheral blood leukocytes were used as the source for germline DNA control. The libraries were prepared using a custom capture panel (Genecast, Beijing, China) that covers the genes associated with cancer diagnosis and prognosis. Afterward, Illumina Novaseq 6000 sequencing systems were used to sequence the captured DNA fragments. The average unique sequence coverage was at least 900× for lymphocytes and 2,000× for tumor tissue samples. Mutect2 was used to detect single nucleotide variants and small indels.

In the mutation calling procedure, each individual's germline mutations were filtered out during tumor-normal paired sample calling. There was a requirement for ≥20 reads of sequencing depth in each somatic mutation region, and ≥5 reads were required to support the variant call. Conversely, the number of reads supporting the variant in the germline data had to be <5, and the sequencing depth had to be ≥20. The variant data were annotated using ANNOVAR (27).

We then filtered out all common germline mutations with a population frequency of ≥1% using the gnomAD,

ExAC, and esp6500 databases. And in order to ensure the data was reliable, common variants and potential background noise from the platform were also excluded. An in-house blacklist from Genecast was used to filter the sequencing-specific errors and background noises. Variants were converted to MAF files using vcf2maf (<https://github.com/mskcc/vcf2maf>). The clinical evidence levels of mutations were annotated with OncoKB MafAnnotator (<https://github.com/oncokb/oncokb-annotator>).

The TMB was defined as the number of somatic coding mutations per megabase of genome examined, which included single-base substitution and indels. And we only considered nonsynonymous mutations and introns (synonymous mutations that do not affect amino acid sequences) were excluded. Specifically, mutations belong to the following ENSEMBL's items: "frame shift del", "frame shift ins", "splice site", "translation start site", "nonsense mutation", "nonstop mutation", "in frame del", "in frame ins", and "missense mutation", which were selected following the instructions of maftools (28).

Statistical analysis

The patient characteristics are presented using descriptive statistics. The continuous variables are presented as the median and interquartile range, and the categorical data are presented as the count and frequency. The comparative analysis of the continuous and categorical variables between the groups was performed with the Wilcoxon rank-sum test for two independent samples and Fisher's exact test, respectively, using the R package ggpubr. The Kaplan-Meier method was used for the survival analysis, and log-rank test was used to test the significance of differences between survival curves. The univariable and multivariable survival analyses were performed with Cox's proportional hazards model to generate estimates of the hazard ratios (HRs) and the corresponding 95% confidence intervals (CIs) using the R package survminer. The Spearman correlation matrix was calculated and plotted using the R package corrplot. P<0.05 was considered significant.

Results

Genomic landscape of early stage LUSC

In this study, a total of 180 patients were enrolled, and their baseline clinicopathological characteristics are set out in *Table 1*. Patients had a median age of 63 years (57–68 years).

Table 1 Baseline clinicopathological characteristics of the included patients (n=180)

Characteristics	Total	PD-L1+ (E1L3N_TC)	PD-L1- (E1L3N_TC)	P value
Age, n (%)				0.09
<65	113 (62.8)	53 (70.7)	60 (57.1)	
≥65	67 (37.2)	22 (29.3)	45 (42.9)	
Sex, n (%)				0.53
Female	10 (5.6)	3 (4.0)	7 (6.7)	
Male	170 (94.4)	72 (96.0)	98 (93.3)	
ECOG PS, n (%)				0.06
0	132 (73.3)	49 (65.3)	83 (79.0)	
1	48 (26.7)	26 (34.7)	22 (21.0)	
Smoking, n (%)				1.00
Never	55 (30.6)	23 (30.7)	32 (30.5)	
Ever	125 (69.4)	52 (69.3)	73 (69.5)	
TNM stage, n (%)				0.86
I/II	135 (75.0)	57 (76.0)	78 (74.3)	
III	45 (25.0)	18 (24.0)	27 (25.7)	
Lymph node invasion, n (%)				0.14
No	141 (78.3)	63 (84.0)	78 (74.3)	
Yes	39 (21.7)	12 (16.0)	27 (25.7)	
Lymph node stage, n (%)				0.27
0	141 (78.3)	63 (84.0)	78 (74.3)	
1	25 (13.9)	7 (9.3)	18 (17.1)	
2	14 (7.8)	5 (6.7)	9 (8.6)	
Differentiation, n (%)				0.18
Low	51 (28.3)	19 (25.3)	32 (30.5)	
Intermediate	119 (66.1)	49 (65.3)	70 (66.7)	
High	10 (5.6)	7 (9.3)	3 (2.9)	
Maximum diameter	4 [2.9–5]	3.5 [2.8–5]	4 [3–5]	0.52
Pleural invasion, n (%)				0.16
No	166 (92.2)	72 (96.0)	94 (89.5)	
Yes	14 (7.8)	3 (4.0)	11 (10.5)	
Venous invasion, n (%)				0.72
0	172 (95.6)	71 (94.7)	101 (96.2)	
1	8 (4.4)	4 (5.3)	4 (3.8)	
CD8 ⁺ TILs (%)	11.5 (4, 24)	17 (5, 30)	9 (3.5, 21)	0.002
SP142_IC (%)	0 (0–0)	0 (0–0)	0 (0–0)	0.017
SP142_TC (%)	0 (0–0)	0 (0–8)	0 (0–0)	<0.001
TMB	9.4 (7.5–13.7)	9.4 (7.6–13.1)	9.4 (7.5–14.9)	0.69

Continuous variables are shown as median and interquartile range, and categorical variables are shown with number and frequency. ECOG PS, Eastern Cooperative Oncology Group performance status; TNM stage, tumor-node-metastasis stage; TILs, tumor-infiltrating lymphocytes; IC, immune cell; TC, tumor cell; TMB, tumor mutation burden; PD-L1, programmed cell death-ligand 1.

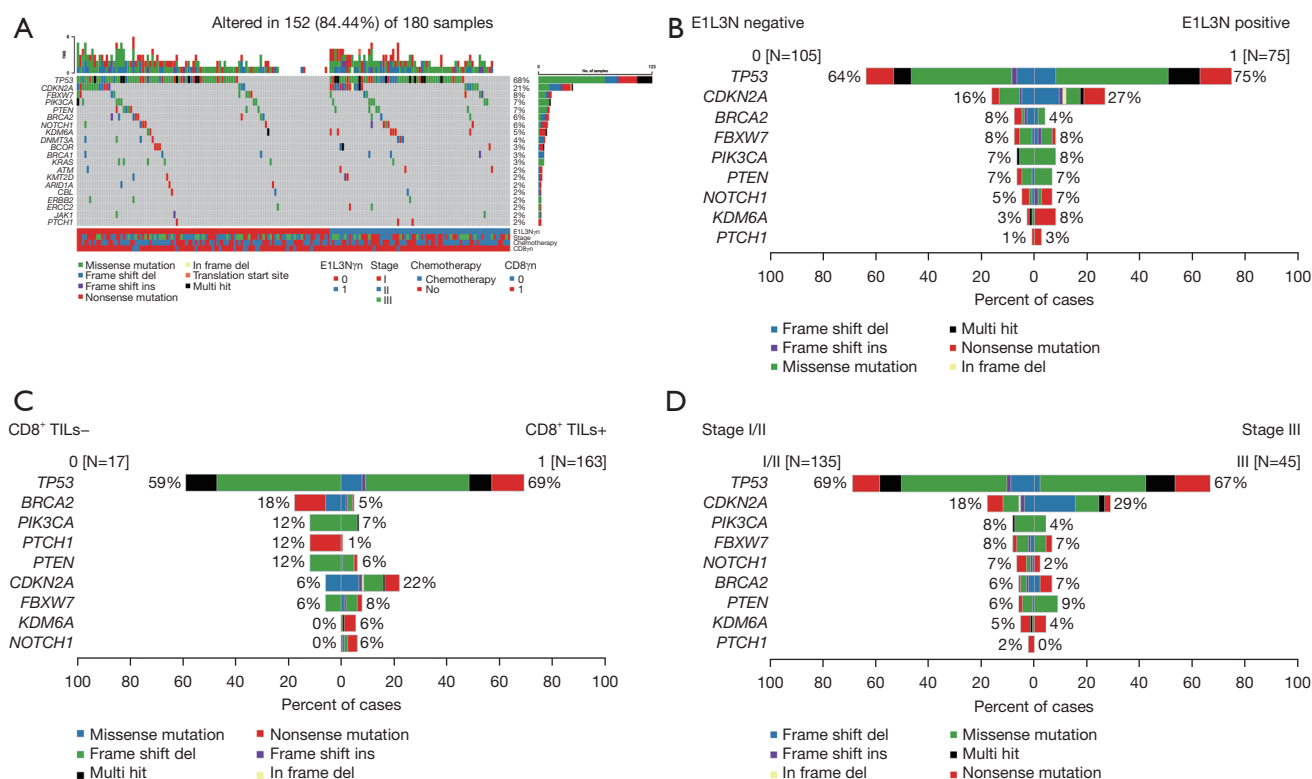


Figure 1 Genomic landscape of early stage LUSC. (A) Identified somatic mutations in all cases. The associations between gene mutations and (B) PD-L1 expression (E1L3N_TC), (C) CD8⁺ TILs infiltration, and (D) tumor TNM stages. TILs, tumor-infiltrating lymphocytes; CD8⁺, cluster of differentiation 8⁺; LUSC, lung squamous cell carcinoma; PD-L1, programmed cell death-ligand 1; TC, tumor cells; TNM stages, tumor-node-metastasis stages.

Of the patients, 170 (94.4%) were male, and 132 (73.3%) had an ECOG PS of 0. Additionally, 135 (75.0%) patients were confirmed to have TNM stage I/II, and most patients (n=125, 69.4%) had a smoking history. Using a cutoff value of 1%, PD-L1+ tumor cells (E1L3N_TC) were observed in 75 (41.7%) patients; a figure higher than that reported for Caucasian LUSC populations (29). In the CHOICE study (which included both Chinese LUSC and LUAD patients), the PD-L1 positive rate was 23.1% using a H-score ≥ 50 , or 63.9% using $>1\%$ positivity in tumor cells as a cutoff; figures consistent with those reported in research on Western populations (30,31). As a control, the clone SP142 PD-L1 antibody was used, and the rate of PD-L1+ immune cells (SP142_IC) was 0 [0, 0] in both groups (PD-L1+/-), and the rate of PD-L1+ tumor cells (SP142_TC) was 0 [0, 8] in the PD-L1+ group (E1L3N_TC) and 0 [0, 0] in the PD-L1- group (E1L3N_TC). The median TMB of both the PD-L1+ group (E1L3N_TC) and PD-L1- group (E1L3N_TC) were 9.4 mut/Mb, and the median rate of the CD8⁺

TILs was 17 [5, 30] in the PD-L1+ group (E1L3N_TC) and 9 [3.5, 21] in the PD-L1- group (E1L3N_TC).

All of the 180 samples were sequenced, and mutations with clinical evidence were identified using the OncoKB database. Altered genes were identified in 152 (84.4%) of the samples (see Figure 1A) and the top 8 altered genes (no less than 5%) were tumor suppressor p53 (*TP53*), cyclin-dependent kinase inhibitor 2A (*CDKN2A*), F-box with 7 tandem WD40 (*FBXW7*), phosphatidylinositol-4,5-bisphosphate 3-kinase catalytic subunit alpha (*PIK3CA*), phosphatase and tensin homolog (*PTEN*), Breast-Cancer susceptibility gene 2 (*BRCA2*), notch homolog protein 1 (*NOTCH1*), and Lysine demethylase 6A (*KDM6A*). This was similar to the significantly mutated genes reported in The Cancer Genome Atlas (TCGA) database, which identified 10 genes [i.e., *TP53*, *CDKN2A*, *PTEN*, *PIK3CA*, Kelch-like ECH-associated protein 1 (*KEAP1*), Mixed Lineage Leukemia 2 (*MLL2*), Human leukocyte antigen A (*HLA-A*), Nuclear factor erythroid 2-related factor 2

Table 2 Univariate and multivariate analyses of clinicopathological characteristics for DFS

Variable	Univariate analysis		Multivariate analysis	
	HR (95% CI)	P value	HR (95% CI)	P value
Age (≥65 vs. <65 y)	1.166 (0.834, 1.632)	0.369		
Sex (male vs. female)	0.891 (0.454, 1.751)	0.738		
ECOG PS (1 vs. 0)	1.103 (0.766, 1.588)	0.599		
Smoking (ever vs. never)	1.036 (0.729, 1.474)	0.842		
TNM stage (III vs. I/II)	1.690 (1.167, 2.446)	0.005*	1.719 (1.181, 2.504)	0.005*
Lymph node invasion (yes vs. no)	1.385 (0.934, 2.053)	0.105		
Lymph node stage (1 vs. 0)	1.464 (0.909, 2.357)	0.245		
Lymph node stage (2 vs. 0)	1.270 (0.700, 2.306)	0.245		
Differentiation (intermediate vs. low)	1.060 (0.733, 1.532)	0.817		
Differentiation (high vs. low)	1.276 (0.596, 2.732)	0.817		
Maximum diameter (≥4 vs. <4)	1.068 (0.979, 1.164)	0.140		
Pleural invasion (yes vs. no)	1.838 (1.035, 3.261)	0.037*	1.751 (0.972, 3.155)	0.062
Venous invasion (yes vs. no)	1.883 (0.877, 4.044)	0.104		
CD8 ⁺ TILs (>0 vs. 0)	0.400 (0.238, 0.6724)	<0.001*	0.433 (0.255, 0.735)	0.002*
TMB (≥9.4 vs. <9.4)	1.253 (0.903, 1.738)	0.177		
PD-L1 (≥1% vs. <1%)	0.615 (0.438, 0.864)	0.005*	0.700 (0.493, 0.993)	0.046*

Variables with a P value <0.05 in the univariate models were analyzed in the multivariate analysis model. *, P<0.05. DFS, disease-free survival; ECOG PS, Eastern Cooperative Oncology Group performance status; TNM stage, tumor-node-metastasis stage; CD8⁺, cluster of differentiation 8⁺; TILs, tumor-infiltrating lymphocytes; TMB, tumor mutation burden; PD-L1, programmed cell death-ligand 1.

(*NFE2L2*), *NOTCH1*, and Retinoblastomal (*RBI*)] with a false discovery rate *Q* value <0.1 (31). Additionally, 14 genes exhibited significant enrichment for the somatic mutation in Caucasians with LUSC (Kadara *et al.* cohort): *TP53*, *MLL2*, *PIK3CA*, *NFE2L2*, *CDH8*, *KEAP1*, *PTEN*, *ADCY8*, *PTPRT*, *CALCR*, *GRM8*, *FBXW7*, *RBI*, and *CDKN2A* (32). In our cohort, the *TP53* mutation was most frequently found in 68% of all cases (TCGA: 81%; Kadara *et al.* cohort: 60%) followed by *CDKN2A* in 21% of all cases. The mutation rates of *TP53* (64% vs. 75%; P=0.145), *CDKN2A* (16% vs. 27%; P=0.095), *BRCA2* (8% vs. 4%; P=0.365), *FBXW7* (8% vs. 8%; P=1.000), *PIK3CA* (7% vs. 8%; P=0.776), *KDM6A* (3% vs. 8%; P=0.167) were comparable between the PD-L1+ and PD-L1- patients (see *Figure 1B*). Similarly, gene alterations, including *TP53* (59% vs. 69%; P=0.416), *BRCA2* (18% vs. 5%; P=0.072), *PIK3CA* (12% vs. 7%; P=0.353), *PTCH1* (12% vs. 1%; P=0.024), *PTEN* (12% vs. 6%; P=0.316), *CDKN2A* (6% vs. 22%; P=0.203), *FBXW7* (6% vs. 8%; P=1.000), and *NOTCH1* (0% vs. 6%; P=1.000), were comparable between

the CD8⁺ TILs+ group and CD8⁺ TILs- group, and only the gene mutation frequency of *PTCH1* was significantly different between the two groups (see *Figure 1C*), and the contingency coefficient of *PTCH1* between CD8⁺ TILs+ group and CD8⁺ TILs- group was 0.247, P=0.001. However, the gene variation rate did not differ significantly between the two groups (TNM stages I/II and III), including *TP53* (69% vs. 67%; P=0.854), *CDKN2A* (18% vs. 29%; P=0.136), *PIK3CA* (8% vs. 4%; P=0.523), *FBXW7* (8% vs. 7%; P=1.000), *NOTCH1* (7% vs. 2%; P=0.455), *BRCA2* (6% vs. 7%; P=1.000), and *PTEN* (6% vs. 9%; P=0.498; see *Figure 1D*).

Effects of clinicopathological characteristics on survival

The univariate and multivariate analyses results are set out in *Table 2*. In the univariate analysis, TNM stage (HR =1.690; P=0.005), pleural invasion (HR =1.838; P=0.037), CD8⁺ TILs (HR =0.400; P<0.001), and PD-L1 (HR =0.615; P=0.005) were significantly associated with DFS.

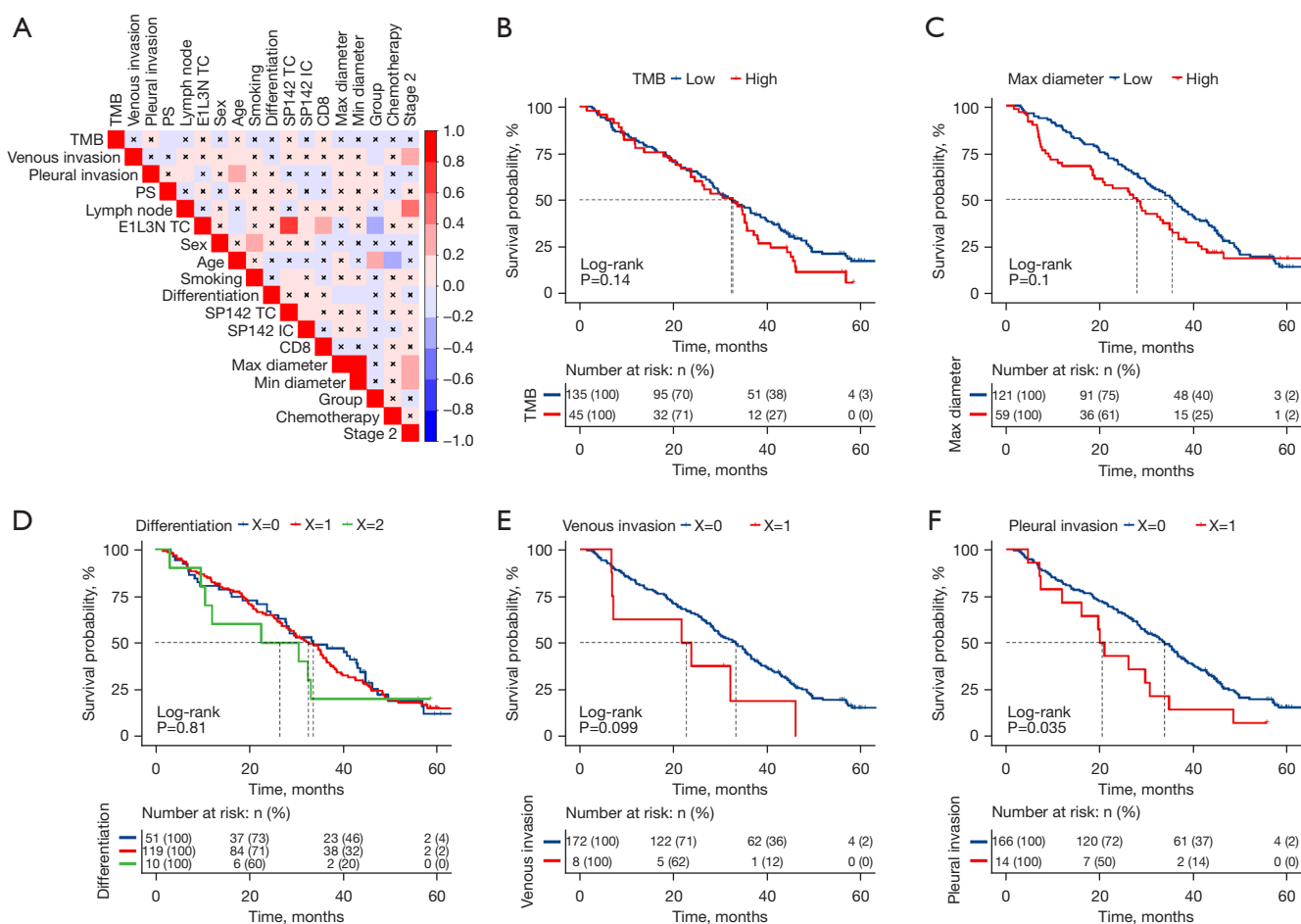


Figure 2 Effects of clinicopathological characteristics on DFS. (A) The correlation matrix and cluster analysis were performed using the clinicopathological characteristics. (B-F) Effects of TMB, maximum diameter, differentiation degree, venous invasion, and pleural invasion on DFS. TC, tumor cell; IC, immune cell; CD8, cluster of differentiation 8; TMB, tumor mutation burden; DFS, disease-free survival.

The multivariate analysis results showed that TNM stage (HR =1.719; P=0.005) was an independent risk factor and both CD8⁺ TILs (HR =0.433, P=0.002) and PD-L1 (HR =0.700, P=0.046) were independent protective factors for longer DFS.

Next, we conducted a survival analysis. The median follow-up time was 105 months, and the median DFS was 33.1 months (95% CI: 28.227, 37.973), while the median OS didn't reach, which maybe because 75% of the patients were stage I/II. Therefore, only DFS was examined in the survival analysis. As Figure 2A showed, a correlation matrix analysis and cluster analysis of the clinical characteristics were performed. The Kaplan-Meier method was used for the continuous variables that were grouped by the first quartile, median, and third quartile to determine the

best cutoff value. The results indicated that patients with different TMB levels (see Figure 2B), maximum diameters (see Figure 2C), differentiation degrees (see Figure 2D), and venous invasion statuses (Figure 2E) had comparable DFS. Notably, pleural invasion (P=0.035) status was significantly correlated with a poorer DFS (see Figure 2F), and high PD-L1 expression on tumor cells tested by the clone E1L3N PD-L1 antibody (E1L3N_TC) (HR =0.615, P=0.0046; see Figure 3A) and CD8⁺ TILs+ (CD8_IC) (HR =0.400, P=0.0014; see Figure 3B) were significantly associated with longer DFS. A further subgroup analysis revealed that both E1L3N_TC (see Figure 3C) and CD8_IC (see Figure 3D) were significantly correlated with the DFS of stage I/II patients, but not the DFS of stage III patients.

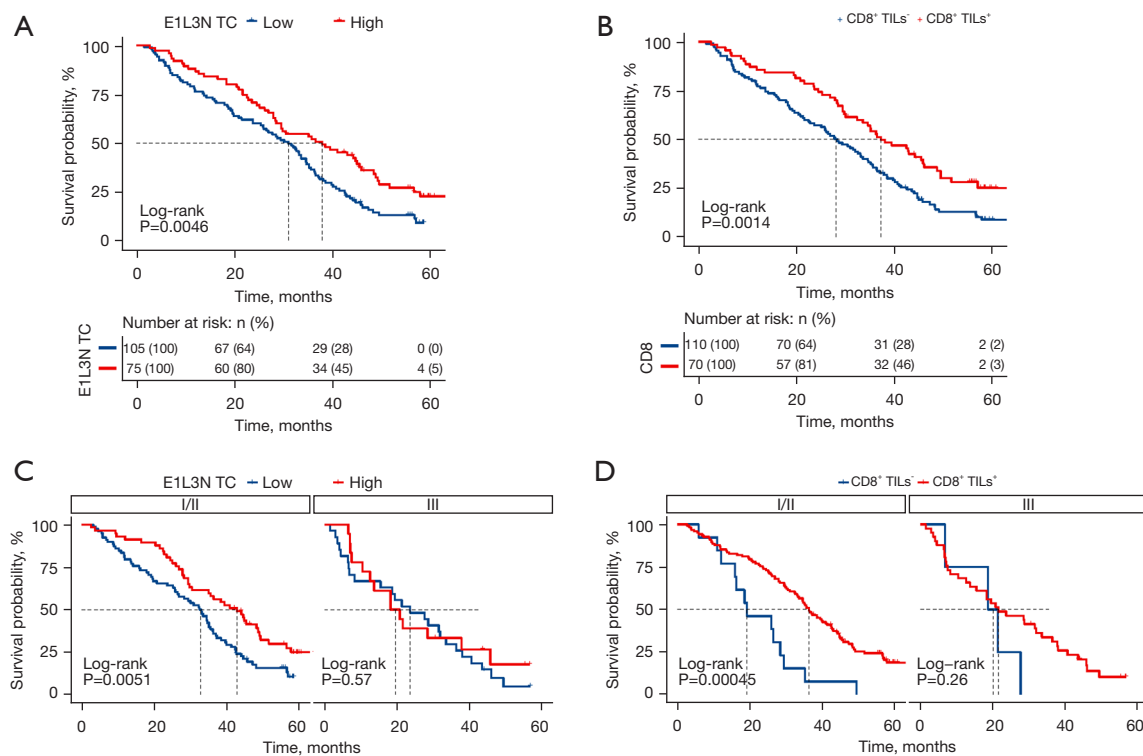


Figure 3 Effects of E1L3N_TC and CD8⁺ TILs on DFS. Kaplan-Meier curves of DFS among all patients in terms of (A) E1L3N_TC and (B) CD8⁺ TILs. Subgroup analysis of DFS among patients with stage I/II or III LUSC in terms of (C) E1L3N_TC and (D) CD8⁺ TILs. TC, tumor cell; CD8, cluster of differentiation 8; DFS, disease-free survival; LUSC, lung squamous cell carcinoma.

Discussion

Lung cancer is one of the most pathogenic and fatal cancer diseases in the world (33), and LUSC is a major pathological subtype of lung cancer. Surgery is the standard treatment for early stage LUSC; however, its recurrence rate remains high after surgery. In the last decade, immunotherapy, especially ICIs that target the PD-1/PD-L1 axis, has brought the treatment strategies of advanced lung cancer into a new era. Exploring the relationship between immune patterns and prognosis is of great significance for neoadjuvant or adjuvant immunotherapy in patients with early LUSC.

We examined 180 samples using targeted sequencing, and the important somatic mutations we reported are consistent with those reported in previous studies (31,32,34,35). Understanding the interaction between the genetic landscape, TME patterns, and clinicopathological parameters may help promote the development of treatment for early stage or advanced non-small cell lung cancer (NSCLC). *PTCH1* gene suppressed the Hedgehog signaling

pathway, which plays an important role in cell embryonic development, by inhibiting a key signal transducer Smoothed receptor (SMO) (36,37). Previous studies have shown that *PTCH1* inhibits the cell cycle and plays a critical role in cancer progression and metastasis (38). Wan *et al.* found that the low expression of *PTCH1* may promote the progression of NSCLC (39). Our results of the sequencing and IHC staining analysis revealed that only *PTCH1* gene mutation frequency was significantly lower in patients with CD8⁺ TILs+. And the results of the Kaplan-Meier survival analysis confirmed that higher CD8 infiltration were significantly correlated with longer DFS. These results suggest that lower *PTCH1* gene mutation and CD8⁺TILs+ may be beneficial background for LUSC patients to have better prognosis.

Higher PD-L1 expression was also significantly with longer DFS and the DFS data was only comparable between high and low TMB groups. Similar to previous reports (40,41), intense lymphocytic infiltration and lower TMB were significantly associated with better DFS. Jiang *et al.* (42) reported that TMB combined with CD8⁺ TILs

and/or PD-L1 could successfully stratify the prognosis of surgically resected LUSC patients and found a significant association between CD8⁺ TILs density and PD-L1 expression. In our study, the multivariate analysis suggested that stage was an independent risk factor for DFS. Thus, we conducted a subgroup analysis to examine the effects of CD8⁺ TILs and PD-L1 expression on DFS based on different TNM stages, and found that the two factors were significantly correlated with the DFS of stage I/II patients but not the DFS of stage III patients. Given these results, a comprehensive analysis of these biomarkers in predicting the prognosis of early LUSC patients is warranted.

In summary, this study explored the gene molecular characteristics of patients with surgically resected LUSC who had not undergone immunotherapy previously and its association with clinicopathological parameters. The results suggested that only *PTCH1* gene mutation frequency was correlated with CD8⁺ TILs density. Intense CD8⁺ TILs density and high PD-L1 expression were associated with a longer DFS. Our findings provide insights into the precision treatment of early LUSC. These preliminary results need to be further validated, and the mechanisms need to be further explored with an enlarged sample size.

Acknowledgments

Funding: This work was supported by the Shanghai Key Specialty of Respiratory Disease and Shanghai Major Disease Multidisciplinary Diagnosis and Treatment Capacity Building Project.

Footnote

Reporting Checklist: The authors have completed the REMARK reporting checklist. Available at <https://jtd.amegroups.com/article/view/10.21037/jtd-22-630/rc>

Data Sharing Statement: Available at <https://jtd.amegroups.com/article/view/10.21037/jtd-22-630/dss>

Conflicts of Interest: All authors have completed the ICMJE uniform disclosure form (available at <https://jtd.amegroups.com/article/view/10.21037/jtd-22-630/coif>). The authors have no conflicts of interest to declare.

Ethical Statement: The authors are accountable for all aspects of the work in ensuring that questions related to the accuracy or integrity of any part of the work are

appropriately investigated and resolved. This study was conducted in accordance with the provisions of the Declaration of Helsinki (as revised in 2013) and was approved by the Ethics Committee of Shanghai Pulmonary Hospital (No. K20-288). Individual consent for this retrospective analysis was waived.

Open Access Statement: This is an Open Access article distributed in accordance with the Creative Commons Attribution-NonCommercial-NoDerivs 4.0 International License (CC BY-NC-ND 4.0), which permits the non-commercial replication and distribution of the article with the strict proviso that no changes or edits are made and the original work is properly cited (including links to both the formal publication through the relevant DOI and the license). See: <https://creativecommons.org/licenses/by-nc-nd/4.0/>.

References

1. Siegel RL, Miller KD, Fuchs HE, et al. Cancer Statistics, 2021. *CA Cancer J Clin* 2021;71:7-33.
2. Gandara DR, Hammerman PS, Sos ML, et al. Squamous cell lung cancer: from tumor genomics to cancer therapeutics. *Clin Cancer Res* 2015;21:2236-43.
3. Reck M, Rabe KF. Precision Diagnosis and Treatment for Advanced Non-Small-Cell Lung Cancer. *N Engl J Med* 2017;377:849-61.
4. Langer CJ, Obasaju C, Bunn P, et al. Incremental Innovation and Progress in Advanced Squamous Cell Lung Cancer: Current Status and Future Impact of Treatment. *J Thorac Oncol* 2016;11:2066-81.
5. Herbst RS, Morgensztern D, Boshoff C. The biology and management of non-small cell lung cancer. *Nature* 2018;553:446-54.
6. Arriagada R, Dunant A, Pignon JP, et al. Long-term results of the international adjuvant lung cancer trial evaluating adjuvant Cisplatin-based chemotherapy in resected lung cancer. *J Clin Oncol* 2010;28:35-42.
7. Herbst RS, Baas P, Kim DW, et al. Pembrolizumab versus docetaxel for previously treated, PD-L1-positive, advanced non-small-cell lung cancer (KEYNOTE-010): a randomised controlled trial. *Lancet* 2016;387:1540-50.
8. Brahmer J, Reckamp KL, Baas P, et al. Nivolumab versus Docetaxel in Advanced Squamous-Cell Non-Small-Cell Lung Cancer. *N Engl J Med* 2015;373:123-35.
9. Antonia SJ, Villegas A, Daniel D, et al. Overall Survival with Durvalumab after Chemoradiotherapy in Stage III NSCLC. *N Engl J Med* 2018;379:2342-50.

10. Borghaei H, Paz-Ares L, Horn L, et al. Nivolumab versus Docetaxel in Advanced Nonsquamous Non-Small-Cell Lung Cancer. *N Engl J Med* 2015;373:1627-39.
11. Forde PM, Chaft JE, Smith KN, et al. Neoadjuvant PD-1 Blockade in Resectable Lung Cancer. *N Engl J Med* 2018;378:1976-86.
12. Han H, Silverman JF, Santucci TS, et al. Vascular endothelial growth factor expression in stage I non-small cell lung cancer correlates with neoangiogenesis and a poor prognosis. *Ann Surg Oncol* 2001;8:72-9.
13. Galon J, Costes A, Sanchez-Cabo F, et al. Type, density, and location of immune cells within human colorectal tumors predict clinical outcome. *Science* 2006;313:1960-4.
14. Pilotto S, Sperduti I, Leuzzi G, et al. Prognostic Model for Resected Squamous Cell Lung Cancer: External Multicenter Validation and Propensity Score Analysis exploring the Impact of Adjuvant and Neoadjuvant Treatment. *J Thorac Oncol* 2018;13:568-75.
15. Fridman WH, Pagès F, Sautès-Fridman C, et al. The immune contexture in human tumours: impact on clinical outcome. *Nat Rev Cancer* 2012;12:298-306.
16. Mlecnik B, Bindea G, Pagès F, et al. Tumor immunosurveillance in human cancers. *Cancer Metastasis Rev* 2011;30:5-12.
17. Zeng Z, Yang F, Wang Y, et al. Significantly different immunoscores in lung adenocarcinoma and squamous cell carcinoma and a proposal for a new immune staging system. *Oncoimmunology* 2020;9:1828538.
18. Stiles BM, Rahouma M, Hussein MK, et al. Never smokers with resected lung cancer: different demographics, similar survival. *Eur J Cardiothorac Surg* 2018;53:842-8.
19. Imai H, Kaira K, Minato K. Clinical significance of post-progression survival in lung cancer. *Thorac Cancer* 2017;8:379-86.
20. Ock CY, Keam B, Kim S, et al. Pan-Cancer Immunogenomic Perspective on the Tumor Microenvironment Based on PD-L1 and CD8 T-Cell Infiltration. *Clin Cancer Res* 2016;22:2261-70.
21. Chalela R, Curull V, Enríquez C, et al. Lung adenocarcinoma: from molecular basis to genome-guided therapy and immunotherapy. *J Thorac Dis* 2017;9:2142-58.
22. Amin MB, Greene FL, Edge SB, et al. The Eighth Edition AJCC Cancer Staging Manual: Continuing to build a bridge from a population-based to a more "personalized" approach to cancer staging. *CA Cancer J Clin* 2017;67:93-9.
23. Armato SG 3rd, Nowak AK. Revised Modified Response Evaluation Criteria in Solid Tumors for Assessment of Response in Malignant Pleural Mesothelioma (Version 1.1). *J Thorac Oncol* 2018;13:1012-21.
24. Takada K, Okamoto T, Toyokawa G, et al. The expression of PD-L1 protein as a prognostic factor in lung squamous cell carcinoma. *Lung Cancer* 2017;104:7-15.
25. Yang H, Shi J, Lin D, et al. Prognostic value of PD-L1 expression in combination with CD8+ TILs density in patients with surgically resected non-small cell lung cancer. *Cancer Med* 2018;7:32-45.
26. Tokito T, Azuma K, Kawahara A, et al. Predictive relevance of PD-L1 expression combined with CD8+ TIL density in stage III non-small cell lung cancer patients receiving concurrent chemoradiotherapy. *Eur J Cancer* 2016;55:7-14.
27. Wang K, Li M, Hakonarson H. ANNOVAR: functional annotation of genetic variants from high-throughput sequencing data. *Nucleic Acids Res* 2010;38:e164.
28. Mayakonda A, Lin DC, Assenov Y, et al. Maftools: efficient and comprehensive analysis of somatic variants in cancer. *Genome Res* 2018;28:1747-56.
29. Yu H, Chen Z, Ballman KV, et al. Correlation of PD-L1 Expression with Tumor Mutation Burden and Gene Signatures for Prognosis in Early-Stage Squamous Cell Lung Carcinoma. *J Thorac Oncol* 2019;14:25-36.
30. Zhang XC, Wang J, Shao GG, et al. Comprehensive genomic and immunological characterization of Chinese non-small cell lung cancer patients. *Nat Commun* 2019;10:1772.
31. Cancer Genome Atlas Research Network. Comprehensive genomic characterization of squamous cell lung cancers. *Nature* 2012;489:519-25.
32. Kadara H, Choi M, Zhang J, et al. Whole-exome sequencing and immune profiling of early-stage lung adenocarcinoma with fully annotated clinical follow-up. *Ann Oncol* 2017;28:75-82.
33. Sung H, Ferlay J, Siegel RL, et al. Global Cancer Statistics 2020: GLOBOCAN Estimates of Incidence and Mortality Worldwide for 36 Cancers in 185 Countries. *CA Cancer J Clin* 2021;71:209-49.
34. Choi M, Kadara H, Zhang J, et al. Mutation profiles in early-stage lung squamous cell carcinoma with clinical follow-up and correlation with markers of immune function. *Ann Oncol* 2017;28:83-9.
35. Okamoto T, Takada K, Sato S, et al. Clinical and Genetic Implications of Mutation Burden in Squamous Cell Carcinoma of the Lung. *Ann Surg Oncol* 2018;25:1564-71.
36. Sriperumbudur A, Breitzig M, Lockey R, et al. Hedgehog: the key to maintaining adult lung repair and regeneration. *J Cell Commun Signal* 2017;11:95-6.

37. Hasanovic A, Mus-Veteau I. Targeting the Multidrug Transporter Ptc1 Potentiates Chemotherapy Efficiency. *Cells* 2018;7:107.
 38. Li Y, Zhang D, Chen C, et al. MicroRNA-212 displays tumor-promoting properties in non-small cell lung cancer cells and targets the hedgehog pathway receptor PTCH1. *Mol Biol Cell* 2012;23:1423-34.
 39. Wan X, Kong Z, Chu K, et al. Co-expression analysis revealed PTCH1-3'UTR promoted cell migration and invasion by activating miR-101-3p/SLC39A6 axis in non-small cell lung cancer: implicating the novel function of PTCH1. *Oncotarget* 2018;9:4798-813.
 40. Owada-Ozaki Y, Muto S, Takagi H, et al. Prognostic Impact of Tumor Mutation Burden in Patients With Completely Resected Non-Small Cell Lung Cancer: Brief Report. *J Thorac Oncol* 2018;13:1217-21.
 41. Brambilla E, Le Teuff G, Marguet S, et al. Prognostic Effect of Tumor Lymphocytic Infiltration in Resectable Non-Small-Cell Lung Cancer. *J Clin Oncol* 2016;34:1223-30.
 42. Jiang T, Shi J, Dong Z, et al. Genomic landscape and its correlations with tumor mutational burden, PD-L1 expression, and immune cells infiltration in Chinese lung squamous cell carcinoma. *J Hematol Oncol* 2019;12:75.
- (English Language Editor: L. Huleatt)

Cite this article as: Cheng X, Wang L, Zhang Z. Prognostic significance of PD-L1 expression and CD8⁺ TILs density for disease-free survival in surgically resected lung squamous cell carcinoma: a retrospective study. *J Thorac Dis* 2022;14(6):2224-2234. doi: 10.21037/jtd-22-630